

Review

# A Picture of Modern Tc-99m Radiopharmaceuticals: Production, Chemistry, and Applications in Molecular Imaging

Alessandra Boschi <sup>1</sup>, Licia Uccelli <sup>2,3</sup> and Petra Martini <sup>2,4,\*</sup>

<sup>1</sup> Department of Chemical and Pharmaceutical Sciences, University of Ferrara, Via Luigi Borsari, 46, 44121 Ferrara, Italy; alessandra.boschi@unife.it

<sup>2</sup> Department of Morphology, Surgery and Experimental Medicine, University of Ferrara, Via Luigi Borsari, 46, 44121 Ferrara, Italy; licia.uccelli@unife.it

<sup>3</sup> Nuclear Medicine Unit, University Hospital, Via Aldo Moro, 8, 44124 Ferrara, Italy

<sup>4</sup> Legnaro National Laboratories, Italian National Institute for Nuclear Physics (LNL-INFN), Viale dell'Università, 2, 35020 Legnaro (PD), Italy

\* Correspondence: petra.martini@unife.it; Tel.: +39-0532-455354

Received: 15 May 2019; Accepted: 19 June 2019; Published: 21 June 2019



**Abstract:** Even today, technetium-99m represents the radionuclide of choice for diagnostic radio-imaging applications. Its peculiar physical and chemical properties make it particularly suitable for medical imaging. By the use of molecular probes and perfusion radiotracers, it provides rapid and non-invasive evaluation of the function, physiology, and/or pathology of organs. The versatile chemistry of technetium-99m, due to its multi-oxidation states, and, consequently, the ability to produce a variety of complexes with particular desired characteristics, are the major advantages of this medical radionuclide. The advances in technetium coordination chemistry over the last 20 years, in combination with recent advances in detector technologies and reconstruction algorithms, make SPECT's spatial resolution comparable to that of PET, allowing <sup>99m</sup>Tc radiopharmaceuticals to have an important role in nuclear medicine and to be particularly suitable for molecular imaging. In this review the most efficient chemical methods, based on the modern concept of the <sup>99m</sup>Tc-metal fragment approach, applied to the development of technetium-99m radiopharmaceuticals for molecular imaging, are described. A specific paragraph is dedicated to the development of new <sup>99m</sup>Tc-based radiopharmaceuticals for prostate cancer.

**Keywords:** technetium-99m; chemistry; radiopharmaceuticals

## 1. Introduction

Molecular Imaging (MI) is a type of medical procedure that provides the visualization, characterization, and measurement of biological processes at the molecular and cellular levels in living systems [1].

Nuclear medicine is a branch of MI that, through the use of radiopharmaceuticals, allows physicians to see and to measure functional, metabolic, chemical, and biological processes within the body and/or to treat malignant tumours, cancer, and other diseases [2–5].

In general, a radiopharmaceutical is a medicinal product that is, usually, administered intravenously to the patient. The radiopharmaceutical is the result of the linkage of two elements, a carrier and at least one radioactive atom that, with its nuclear properties, defines the diagnostic and/or therapeutic nature of the radioactive compound. The carrier plays an important role in the selective transport of the radionuclide to a specific biological target (Figure 1).

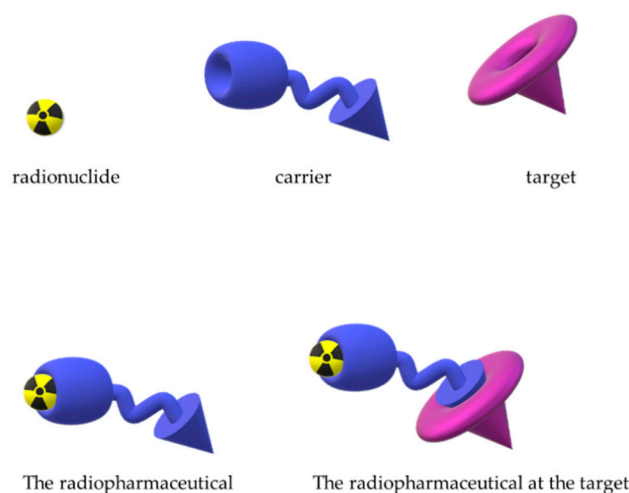


**Figure 1.** Schematic representation of linkage of the carrier and the radioactive atom to form the radiopharmaceutical that interacts with a specific biological target.

Radioactive atoms decay through a nuclear process that leads to the production of  $\gamma$ -rays used in the diagnostic imaging field. In this case, the radioactivity coming from the radiopharmaceutical, carrying the diagnostic information outward from the body, is detected and transformed in a very precise picture of the radiopharmaceutical's distribution in the body by means of so-called "gamma cameras" working with sophisticated computerized algorithms. On the contrary, radionuclides decaying through the emission of massive particles, such as electrons or alphas, can be used in nuclear medicine for radionuclide therapy to treat certain types of cancer and other diseases [6–8].

Ideally, for diagnostic nuclear medicine imaging applications, each nuclear decay should yield a monochromatic gamma-ray in the energy range 100–600 keV, and the half-life of the radionuclide should be on the order of a few hours to avoid unnecessary exposure to radiation. Radiopharmaceuticals for single-photon computed tomography (SPECT) are generally composed of single small molecules (the size can range from  $10^{-12}$  to  $10^{-6}$  m) radiolabelled with a gamma-emitting isotope, such as indium-111, iodine-123, gallium-67, or technetium-99m.

Advanced methods to specifically and selectively incorporate medical radionuclides, such as radiometals, into targeting vectors, based on an improved understanding of their coordination chemistry and the development of creative labelling strategies, are the core of modern radiopharmaceutical research [9–11].

Among the SPECT isotopes currently in use, technetium-99m has become the workhorse of diagnostic nuclear medicine and technetium-99m-based radiopharmaceuticals are still the most used radioactive chemical compounds in hospitals' clinical practice [12–15]. The main reasons for  $^{99m}\text{Tc}$ 's continuing usage are its ideal nuclear properties and its convenient supply method through a commercial generator system. Technetium-99m decays through the emission of 140 keV  $\gamma$ -rays (89% abundance), which is ideal for imaging with medical gamma cameras, and can be administered to patients in low-radiation doses. Moreover, its 6-h half-life is sufficient for the preparation of  $^{99m}\text{Tc}$  radiopharmaceuticals (in hospitals or centralized radiopharmacies), their possible distribution, the performance of quality controls, administration to the patient, accumulation in the target organ, and image acquisition. Even if the use of radiopharmaceuticals labelled with positron emitters radionuclides challenged the field of SPECT tracers, over 70% of diagnostic investigations are still performed with this single isotope for imaging of bone, renal, hepatic, hepatobiliary, cardiac, and oncological diseases or other pathologies. Until some years ago, the inferior sensitivity, temporal and spatial resolution of SPECT cameras compared to positron emission tomography (PET) cameras, together with the complex and contrived inorganic chemistry of this metal, were considered key problems in the development of new technetium-99m compounds for the imaging of more specific molecular targets [16].

Advances in technetium chemistry over the last 20 years have facilitated the development of new technetium radiopharmaceuticals with great potential in clinical practice. In addition, recent advances in detector technologies and reconstruction algorithms clearly showed that the spatial resolution of SPECT is approaching that of PET without a concomitant decrease in sensitivity. In particular, novel multi-pinhole collimators, coupled with cadmium zinc telluride (CZT) solid-state photon detectors to further improve image quality and reduce scanner size, reduce the imaging time and radiation dose. The new SPECT scanners have demonstrated up to a 7-fold increase in photon sensitivity and an up to 2-fold improvement in image resolution. Furthermore, the adoption of CZT involves a superior energy resolution compared to a conventional gamma camera [17].

The above considerations lead us to believe that  $^{99m}\text{Tc}$ -radiopharmaceuticals will continue to play an important role in nuclear medicine and MI. The versatile chemistry of technetium-99m is a major advantage in radiopharmaceutical development.

The aim of this review is to describe and report the most efficient labelling methods to produce modern technetium-99m radiopharmaceuticals for nuclear medicine. Highly specific activities needed for targeting low-concentration targets are easily achievable through advanced chemical procedures involving the  $^{99m}\text{Tc}$ -metal fragment approach. A section is dedicated to the development of new  $^{99m}\text{Tc}$ -based radiopharmaceuticals for prostate cancer.

## 2. Technetium-99m Production Routes

Technetium-99m is easily produced by the decay of the parent molybdenum-99 by eluting compact and transportable  $^{99}\text{Mo}/^{99m}\text{Tc}$  generator systems that are almost always available in nuclear medicine departments. The generator system is a simple apparatus composed of an alumina column on which the  $^{99}\text{Mo}$  is absorbed in the chemical form of molybdate  $[\text{}^{99}\text{Mo}]\text{MoO}_4^{2-}$ . The  $^{99}\text{Mo}$  decays into  $^{99m}\text{Tc}$  leads to the formation of pertechnetate  $[\text{}^{99m}\text{Tc}]\text{TcO}_4^-$ , which is less tightly bound to the alumina column because of its single negative charge compared to the double negative charge of molybdate.  $[\text{}^{99m}\text{Tc}]\text{NaTcO}_4$  can be easily eluted from the column with a saline solution thanks to the depression caused by an under-vacuum vial appositely inserted in the pertechnetate collecting area (Figure 2). The obtained sodium  $^{99m}\text{Tc}$ -pertechnetate is ready for injection or for the preparation of other radiopharmaceuticals [18,19].

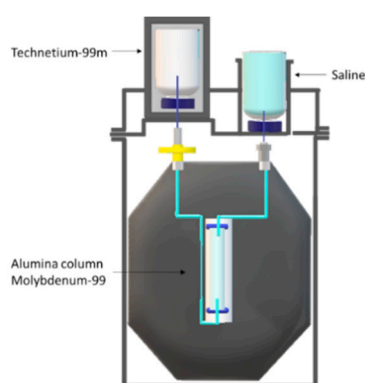


Figure 2. Schematic representation of the  $^{99}\text{Mo}/^{99m}\text{Tc}$  generator system.

The worldwide demand for molybdenum-99 is satisfied by nuclear reactors via the  $^{235}\text{U}(\text{n,f})^{99}\text{Mo}$  fission route on Highly Enriched Uranium targets (HEU, enrichment over 80% in  $^{235}\text{U}$ ). Alternatively, molybdenum-99 can be produced by bombarding molybdenum-98 with high-intensity neutrons to generate sufficient amounts of molybdenum-99 [20].

Nuclear reactors involved in the supply of this isotope are listed in Table 1. In the last decade, they have suffered planned and unplanned shutdowns for maintenance or breakdowns, causing, first in 2009 and then in 2012 and 2013, a shortage in Mo-99 production and therefore in Tc-99m's availability for clinical studies. Recently, significant interruptions in the supply of technetium-99m

occurred in 2016 and 2018, the years when the French OSIRIS and Canadian NRU reactors, respectively, stopped operating.

**Table 1.** Nuclear reactors involved in  $^{99}\text{Mo}$  supply for generator medical devices.

Reactors	Countries	Six-Day GBq/Mo-99 GBq/year	Start of Service	End of Service
LVR-15	Czech Republic	3330000	1957	2028
MARIA	Poland	3515000	1974	2030
OPAL	Australia	3420650	2007	2055
HFR	The Netherlands	8946600	1961	2024
BR2	Belgium	6060600	1961	>2026
RA-3	Argentina	680800	1967	2027
SAFARI-1	South Africa	4835900	1965	2030

In addition to the reactors reported in Table 1, smaller amounts of molybdenum-99 are produced in the RBT-6 and RBT-10 reactors in Russia: irradiating HEU targets have a production capacity of 37,000 GBq/week, and WWR-c has an available production capacity of 12,950 GBq/week. All Mo-99 suppliers except those in Russia produce molybdenum-99 using LEU targets or are in the final stages of converting production from HEU to LEU (Low Enriched Uranium, enrichment below 20% in  $^{235}\text{U}$ ) targets [21].

The supply of molybdenum-99 and technetium-99m is particularly sensitive to reactor shutdowns because, after production, they cannot be stored for future needs due to their short half-lives. Several alternative production routes have been evaluated and some of them have become reliable thanks to the worldwide research efforts of the last 10 years [22–25]. Alternative strategies for the production of molybdenum-99 include the use of linear accelerators, where a molybdenum-100 source is irradiated with gamma rays, as the  $^{100}\text{Mo}(\gamma, n)^{99}\text{Mo}$  reaction [26].

The direct production of  $^{99\text{m}}\text{Tc}$  on cyclotrons, involving the proton bombardment of a solid  $^{100}\text{Mo}$  source in the  $^{100}\text{Mo}(p, 2n)^{99\text{m}}\text{Tc}$  reaction, is now a reality [23,27,28].

A list of various cyclotron and non-cyclotron production routes is given in Table 2.

**Table 2.** Tc-99m alternative production routes.

Reactor Based	Accelerator Based
LEU- $^{235}\text{U}(n, f)^{99}\text{Mo}$	$^{238}\text{U}(\gamma, f)^{99}\text{Mo}$
nat, $^{98}\text{Mo}(n, \gamma)^{99}\text{Mo}$	$^{96}\text{Zr}(\alpha, n)^{99}\text{Mo}$
	$^{100}\text{Mo}(\gamma, n)^{99}\text{Mo}$
	$^{100}\text{Mo}(p, pn)^{99}\text{Mo}$
	$^{100}\text{Mo}(p, 2n)^{99\text{m}}\text{Tc}$

### 3. Chemical Approaches to Bioactive Molecule Labelling with Technetium-99m

In the last decay, the labelling of targeting vectors has become the main object of modern radiopharmaceutical research. Technetium is a transition metal and, as such, presents a major disadvantage with respect to other radionuclides in combining with biologically active molecules. For example,  $^{99\text{m}}\text{Tc}$  cannot be a substitute for a carbon or a hydrogen atom in a targeting molecule, as happens for the labelling with carbon-11, or fluorine-18 and iodine-123 respectively. The development of technetium imaging agents requires both a familiarity with the coordination chemistry of the group 7 metals and an understanding of the design of suitable ligands that provide robust molecular imaging probes. Deep knowledge of inorganic chemistry allows for developing convenient approaches to introduce stable technetium-99m into a bioactive molecule with the aim of not affecting its bioactivity. A number of inorganic technetium functional groups, also called “cores” or “metal fragments,” have been identified so far (Figure 3). These groups are chemical motifs comprising a characteristic arrangement of atoms bonded to the metallic centre and determining the formation of a variety of coordination complexes and molecular geometries. They can be prepared in physiological solution, have technetium

in a reduced oxidation state, and have labile coordination positions, which can be conveniently exploited to introduce the selected bioactive molecule. As previously described, technetium-99m, whether produced by a  $^{99}\text{Mo}/^{99\text{m}}\text{Tc}$  generator or by a cyclotron, is obtained as  $[\text{}^{99\text{m}}\text{Tc}]\text{NaTcO}_4$  in a physiological solution. Consequently, in order to link the radionuclide to a bioactive molecule, the Tc(VII) metal must be reduced to a suitable oxidation state in the presence of appropriate ligands.

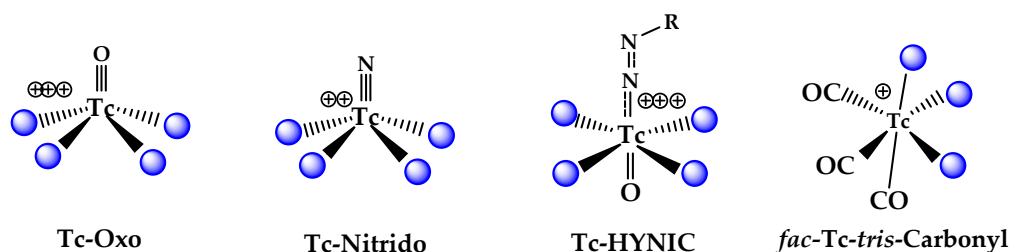


**Figure 3.** Inorganic technetium functional groups useful for labelling bioactive molecules. HYNIC=6-hydrazinonicotinamide.

The metal fragments reported in Figure 3, in combination with an appropriate set of coordinating atoms, provide an effective strategy for tethering a biologically active moiety with a technetium-99m complex. The metal fragment strategy mainly involves a two-component system composed of (1) the radioactive metal fragment and (2) an appropriate chelating group eventually bound to the selected bioactive molecule through a spacer group. The high affinity of the precursor metal fragment for the specific binding sites on the bioactive ligand allows for obtaining a conjugate complex resulting from the fitting of the two carefully selected molecular building blocks (Figure 4).



**Figure 4.** Schematic representation of the metal fragment strategy for bioactive molecule labelling.

In the following section, descriptions of complexes containing the most important technetium functional groups are given. Some of these complexes are also examples of  $^{99\text{m}}\text{Tc}$ -radiopharmaceuticals that have been employed in clinical studies or are currently used as diagnostic agents in clinical practice.

### 3.1. The $^{99\text{m}}\text{Tc(V)}$ -Oxo Core

The  $^{99\text{m}}\text{Tc(V)}$ -oxo core represents the most extensively studied metal fragment. Complexes based on this core are generally pentacoordinated, adopting square pyramidal geometry with the  $\pi$ -bonding oxo-group in the apical position. Due to the strong *trans* influence of the oxo-group, six coordinated technetium-oxo compounds are relatively uncommon. The oxo-core is stabilized by  $\sigma$ - and  $\pi$ -donating atoms coming from amino, amido, and thiolate ligands, as well as the tetradentate ligands of the N4-xSx class [29–32].

These ligands are extremely efficient at forming more stable  $^{99\text{m}}\text{Tc}$ -oxo complexes compared with those derived from bidentate ligands. These compounds can be prepared through the direct reduction of the  $^{99\text{m}}\text{Tc}$ -pertechnetate anion in the presence of tin chloride, which is the ubiquitous preliminary step in the preparation of conventional  $^{99\text{m}}\text{Tc}$ -radiopharmaceuticals, or via a ligand exchange reaction with  $[\text{}^{99\text{m}}\text{Tc}]\text{Tc-glucoheptonate}$  (Figure 5).

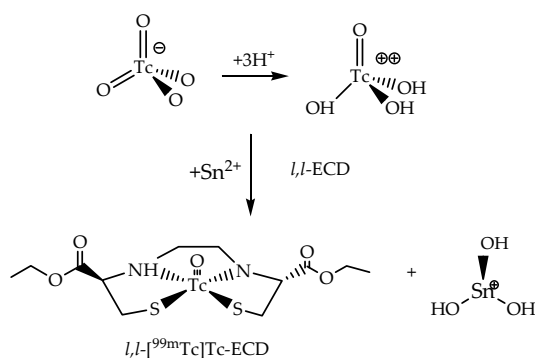


**Figure 5.** Reaction scheme of the preparation of the technetium-99m *N,N*-1,2-ethylene diylbis-*L*-cysteine diethyl ester dihydrochloride from  $^{99m}\text{Tc}$ -pertechnetate.

A representative example is provided by the complex technetium-99m *N,N*-1,2-ethylene diylbis-*L*-cysteine diethyl ester dihydrochloride (*L,L*- $^{99m}\text{Tc}$ ]-Tc-ECD), a brain perfusion imaging agent on the market with the name Neurolite<sup>®</sup>. The complex is neutral and formed by multiple  $\text{Tc}\equiv\text{O}$  bonds coordinated by a tetradentate ligand with two nitrogen and two sulphur donor atoms in a square/pyramidal arrangement. The high symmetry makes the complex hydrophobic. Because of its lipophilicity, it can cross the blood-brain barrier (BBB). The mechanism of brain localization is based on the transformation by esterase enzymes of one of the lateral ester groups ( $-\text{COOEt}$ ) in a carboxylic group ( $-\text{COOH}$ ), with the subsequent formation of a negatively charged more hydrophilic compound that is unable to cross the BBB and thus is trapped. It is important to note that only  $^{99m}\text{Tc}$ -ECD having a *l,l* configuration undergoes ester hydrolysis, making this compound a true metabolic marker of the brain's esterase enzymes.

Mixed aminothiols-based chelators, most notably  $\text{N}_2\text{S}_2$  [e.g., bis(aminoethanethiol) (BAT)] and  $\text{N}_3\text{S}$  [e.g., mercaptoacetylglucylglycylglycine ( $\text{MAG}_3$ )], have been used to label a selected bioactive molecule with technetium-99m [33–37]. These tetradentate chelating systems allow us to produce more stable  $\text{Tc(V)}$ -oxo complexes in comparison with those produced with similar bidentate chelators.

Representative examples from this class of compounds are  $^{99m}\text{Tc}$ -TRODAT-1, a probe for the diagnosis of Parkinson's disease, and  $^{99m}\text{Tc}$ -Depreotide (P829), a  $\text{Tc(V)}$ -oxo somatostatin analogue complex [38–42]. TRODAT-1 (Figure 6) is currently considered a useful imaging agent for the early detection of Parkinson's disease, where a phenyltropane pharmacophore is used as a targeting vector for specific monoamine transporter proteins, and the  $\text{N}_2\text{S}_2$  chelate system, connected to the tropane molecule, has been introduced to coordinate the technetium-oxo core without affecting the affinity for the biological target.

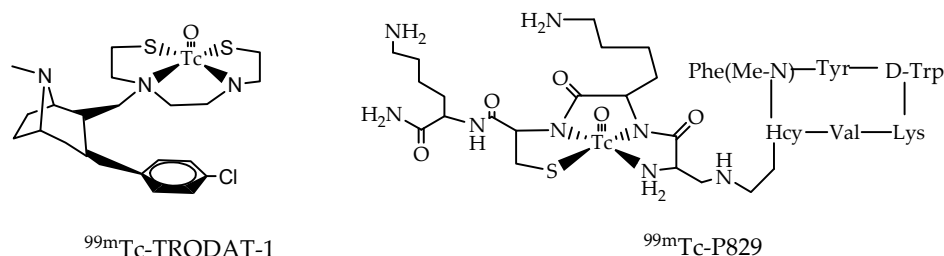


**Figure 6.** Chemical structure of the  $^{99m}\text{Tc}$ -TRODAT-1 and  $^{99m}\text{Tc}$ -Depreotide (P829) radiopharmaceuticals.

Likewise, a tripeptide chain provides a  $\text{N}_3\text{S}$  binding group for  $(\text{Tc}\equiv\text{O})^{3+}$  core in the  $^{99m}\text{Tc}$ -Depreotide radiopharmaceutical (Figure 6) and the bioactive part of the original octreotide structure has been modified to eliminate the disulphide bridge, which would be reduced during the formation of the  $(\text{Tc}\equiv\text{O})^{3+}$  core from the generator-eluted  $^{99m}\text{Tc}$ -pertechnetate.

### 3.2. The $^{99m}\text{Tc(V)}$ -Hydrazido Metal Fragment

Metalorganohydrazine chemistry is an alternative approach to the design of radiopharmaceuticals based on a stable and substitution inert  $^{99m}\text{Tc}$ -metal fragment [43].  $^{99m}\text{Tc}$ -hydrazido metal fragment is formed by a technetium-HYNIC (HYNIC = 6-hydrazinonicotinamide) core composed of the metal in the V oxidation state and occupying the ligand one or two coordination sites. HYNIC ligands are particularly convenient for radiolabelling biomolecules, with  $^{99m}\text{Tc}$  being the active ester most readily combined with small molecules, proteins, or different targeting vectors. However, even if the metal-organohydrazino unit can be easily prepared from the metal-oxo core by a simple condensation reaction, the intimate details of the chemistry are more complex and dependent upon reaction conditions and the presence of co-ligands, which can influence the stability, hydrophilicity, and pharmacokinetics of the resulting  $^{99m}\text{Tc}$ -compounds [44].

A large number of co-ligands have been tested, including ethylenediaminediacetic acid (EDDA), tricine, glucoheptonate, mannitol, thiolates, glucamine, and phosphines forming different binary and ternary systems [45]. The EDDA co-ligand is in general preferred to tricine when preparing  $^{99m}\text{Tc}$ -HYNIC complexes with higher stability in vivo and fewer isomeric forms. Unfortunately, while many efforts have been made to completely establish the identities of these complexes, the chemistry remains unclear. The dependence of the coordination chemistry on the reaction condition of this technology has led to a certain difficulty in the development of  $^{99m}\text{Tc}$ -HYNIC radiopharmaceuticals; moreover, the increasing regulators' requirements of providing fully characterized products does not seem to have promoted HYNIC inclusion in clinical practice. Nevertheless, a wide range of bioactive molecules have been labelled with the HYNIC strategy, among which the most investigated are undoubtedly the somatostatin derivatives for neuroendocrine tumour (NETs) imaging. Most published data concern the commercially available  $^{99m}\text{Tc}$ -[HYNIC, Tyr(3)]octreotide ( $^{99m}\text{Tc}$ -HYNIC-TOC, Figure 7) prepared through a two-vial kit formulation containing EDDA as a co-ligand [46–48].

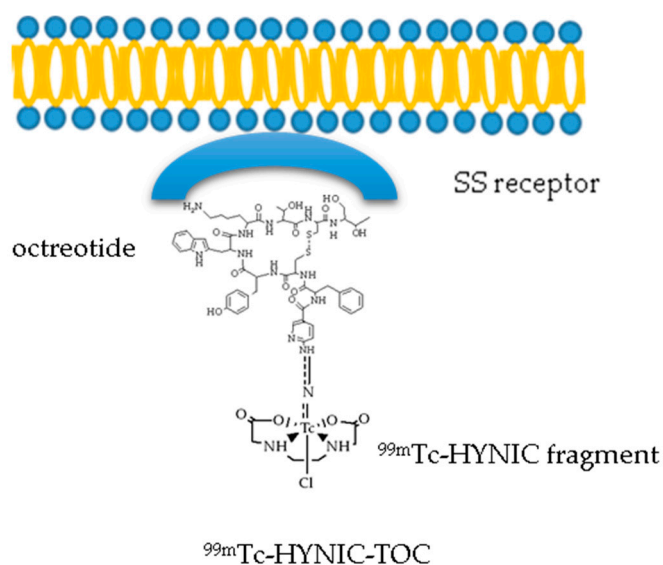


**Figure 7.** The figure illustrates the chemical structure of the complex  $^{99m}\text{Tc}$ -HYNIC-TOC, an imaging agent for neuroendocrine tumours.

The complex is formed by a technetium atom bound to a ligand composed of two functional parts, and a HYNIC group linked to an octapeptide. The EDDA ancillary ligand is required to stabilize the coordination geometry.  $^{99m}\text{Tc}$ -HYNIC-TOC represents a selective receptor imaging agent for neuroendocrine tumours and, even if the true molecular structure of  $^{99m}\text{Tc}$ -HYNIC-TOC is not exactly determined, its biological properties can be understood by considering the bioactive group

octreotide and selectively targeting the somatostatin receptors (SSR) overexpressed on the membranes of neuroendocrine tumours.

This tracer showed greater sensitivity compared to  $^{111}\text{In}$ -octreotide, such as specific and high receptor affinity, good biodistribution, faster renal excretion, lower radiation exposure, and high imaging quality as well as the superior capability of  $^{99\text{m}}\text{Tc}$ -TOC to visualize extrahepatic lesions [49].

### 3.3. The $^{99\text{m}}\text{Tc}(\text{N})\text{PNP}]^{2+}$ Metal Fragment

The nitride technetium mixed ligand complexes  $^{99\text{m}}\text{Tc}[\text{Tc}(\text{N})(\text{PNP})\text{Cl}_2]$  provide a further example of the metal fragment approach, where the  $\text{Tc}(\text{N})$  group is coordinated to a chelating diphosphine ligand of the PNP type and the pentacoordinated geometry is saturated by two chloride atoms. These atoms can be easily replaced by bidentate ligands ( $Y\sim Z$ ) having in their molecular structure electron-rich coordinating atoms ( $Y, Z$ ) highly reactive towards the electrophilic  $^{99\text{m}}\text{Tc}(\text{N})(\text{PNP})]^{2+}$  metallic block to afford the asymmetrical complexes  $^{99\text{m}}\text{Tc}(\text{N})(\text{PNP})(Y\sim Z)]^{0/+}$  [50,51]. From this class of asymmetrical complexes, a novel class of myocardial tracers exhibiting superior qualities was obtained, among which  $^{99\text{m}}\text{Tc}$ -N-DBODC and  $^{99\text{m}}\text{Tc}$ -N-MPO are the most representative (Figure 8) [52,53].

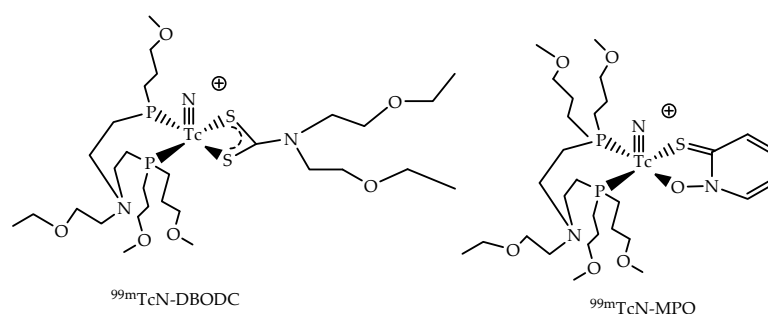


**Figure 8.** Chemical structure of two not-commercial imaging agents for the myocardial perfusion,  $^{99\text{m}}\text{Tc}$ -N-DBODC and  $^{99\text{m}}\text{Tc}$ -N-MPO.

The first compound is prepared through a two-vial kit formulation following a two-step preparation procedure. To the first vial, the generator eluted  $^{99\text{m}}\text{Tc}$ -pertechnetate is added in the presence of  $\text{SnCl}_2$  and succinic dihydrazide (SDH), required to form the  $\text{Tc}\equiv\text{N}$  group. The second vial contains the sodium salt of DBODC (bis-N-ethoxyethyl-dithiocarbamate), the bis(dimethoxypropylphosphinoethyl)-ethoxyethylamine [PNP5;  $(\text{CH}_3\text{OC}_3\text{H}_6)_2\text{P}(\text{CH}_2)_2\text{-N}(\text{C}_2\text{H}_4\text{-OCH}_2\text{CH}_3)\text{-(CH}_2)_2\text{P}(\text{C}_3\text{H}_6\text{OCH}_3)_2$ ], and  $\gamma$ -cyclodextrin, used as a solubilizing agent for the diphosphine ligand. After the reconstitution of the contents of the second lyophilized vial with saline, a part of the resulting solution is added to the first vial and heated at  $100\text{ }^\circ\text{C}$  for 15 min to obtain the final  $^{99\text{m}}\text{Tc}$ -N-DBODC compound with yield  $>95\%$ . A similar procedure is applied to the preparation of the cationic nitride complex  $\text{Tc}$ -N-MPO ( $[(^{99\text{m}}\text{Tc-N}(\text{mpo})(\text{PNP5})]^{+}$ : mpo = 2-mercaptopyridine oxide).  $^{99\text{m}}\text{Tc}$ -N-MPO showed favourable biodistribution properties and myocardial uptake with rapid liver clearance in Sprague-Dawley rats [52,53].

The  $^{99\text{m}}\text{Tc}(\text{N})\text{PNP}]^{2+}$  metal fragment has been efficiently employed for connecting a bioactive molecule with technetium-99m, providing that the biomolecule includes the appropriate set of coordinating atoms. In particular, it was found that the amino acid cysteine shows excellent coordinating properties toward the electrophilic  $^{99\text{m}}\text{Tc}(\text{N})\text{PNP}]^{2+}$  metal fragment, either through the  $(\text{NH}_2, \text{S}^-)$  pair or the  $(\text{O}^-, \text{S}^-)$  pair alternatively, giving rise to highly specific and quantitative reactions. Therefore, a selected bioactive molecule, such as a peptide or a small protein, can be conveniently combined with a cysteine residue through the terminal carboxylic group to form the corresponding COO-functionalized N,S-cysteine ligand or through the terminal amino group to give an N- functionalized O,S-cysteine ligand. The resulting bioactive cysteine derivative is then reacted with  $^{99\text{m}}\text{Tc}(\text{N})\text{PNP}]^{2+}$  to produce the mixed  $^{99\text{m}}\text{Tc}(\text{N})\text{PNP-cysteine-bioactive}]^{0/+}$  complex. This approach has been used for the preparation



of receptor-specific complexes for imaging benzodiazepine receptors and receptor-specific tracers for 5HT1A receptors [54,55].

### 3.4. The [ $^{99m}\text{Tc}][\text{Tc}(\text{CO})_3]^+$ Metal Fragment

The core [ $^{99m}\text{Tc}][\text{Tc}(\text{CO})_3]^+$  is a chemically robust organometallic moiety formed by technetium in the I oxidation state coordinated to three carbonyl groups. The precursor [ $^{99m}\text{Tc}][\text{Tc}(\text{CO})_3(\text{H}_2\text{O})_3]^+$  can be readily prepared from the generator-eluted pertechnetate under the reducing conditions developed by Alberto et al. [56–58].

A large number of different Tc(I) complexes can be prepared starting from this stable water-soluble synthon, because the water ligands can be easily replaced by a variety of donor groups [59,60].

High yields of the [ $^{99m}\text{Tc}][\text{Tc}(\text{CO})_3(\text{H}_2\text{O})_3]^+$  metal fragment are obtained in a single-step procedure in the presence of the appropriate buffers, via the reduction of [ $^{99m}\text{Tc}][\text{TcO}_4]^-$  by potassium boranocarbonate  $\text{K}_2[\text{BH}_3\text{CO}_2]$ , which also acts as a source of carbonyl ligands. With the aim of making this labelling chemistry readily accessible, a kit-based formulation for producing [ $^{99m}\text{Tc}][\text{Tc}(\text{CO})_3(\text{H}_2\text{O})_3]^+$  synthon is available under the name IsoLink.

When the metal has a  $d^6$  low spin configuration, the complexes containing the [ $^{99m}\text{Tc}][\text{Tc}(\text{I})(\text{CO})_3]^+$  core are typically inert and maintain their integrity under different reaction conditions. While the robustness of complexes is purely kinetic, essentially all types of donor atoms have been used and numerous examples of bidentate and tridentate chelators have been reported, including derivatives that can be linked to targeting molecules [61]. As opposed to the traditional  $^{99m}\text{Tc}(\text{V})$ -oxo approach, where the choice of ligand is quite limited, for [ $^{99m}\text{Tc}][\text{Tc}(\text{I})(\text{CO})_3]^+$  almost any monodentate, bidentate, or tridentate donor ligands can be used. Among them, anionic bidentate ligands are more efficient than neutral ones, and tridentate ligands react much faster than bidentate ones, providing the additional advantage of shielding the metal centre from cross-reactions, as often occurs for the [ $^{99m}\text{Tc}(\text{CO})_3(\text{H}_2\text{O})(\text{B})]^+$  and [ $^{99m}\text{Tc}(\text{CO})_3\text{Cl}(\text{B})]^+$  complexes ( $\text{B}$ , bidentate ligand). The most studied tridentate ligands are aliphatic triamines, trithiacyclonane, bis-benzimidazole amine, pyrazolyl borates, and histidine derivatives, which can be conveniently modified to provide complexes with an anionic, cationic, or neutral overall charge and specific pharmacokinetic profiles to achieve the desired biodistribution when the [ $^{99m}\text{Tc}][\text{Tc}(\text{I})(\text{CO})_3]^+$  is incorporated into targeting vectors. Of these ligands, the histidine (his) derivative can be easily connected to biomolecules through the introduction of an acetic acid group at  $\text{N}^\epsilon$  in histidine to yield a  $\text{N}^\alpha$  carboxylate histidine ready to be condensed to a selected biomolecule. The use of histidine has the additional advantage of not being sensitive to reduction and the resulting [ $^{99m}\text{Tc}][\text{Tc}(\text{CO})_3(\text{his})]$  can be prepared in a single reaction step from  $^{99m}\text{Tc}$ -pertechnetate.

## 4. The Metal Fragments Approach in the Development of New $^{99m}\text{Tc}$ -Based Radiopharmaceuticals for Prostate Cancer

Prostate-specific membrane antigen (PSMA), a glutamate carboxypeptidase enzyme overexpressed in 95% of advanced prostate cancer (PCa) cases, is a molecular target for the imaging and radionuclide therapy of PCa using specific radiopharmaceuticals. In particular, the inhibition of its activity has been attributed to the urea-based Lys(b-naphthyl alanine)-NH-CO-NH-Glu(Lys(Nal))-Urea-Glu fragment, which, interacting electrostatically with the active peptide sites of the enzyme, has been shown to image advantageously PSMA-expressing in PCa [62]. Furthermore, when the expression levels in healthy tissue are low, PSMA has the potential for high-dose radiotherapeutic treatment, with minimized radioactivity-related side effects. Recent studies on  $^{177}\text{Lu}$ -PSMA-617 have demonstrated a high tumour to normal tissue uptake, with prolonged retention of radionuclides in tumour-bearing areas in men with metastatic prostate cancer [63–66].

Before therapeutic treatment, the imaging of radiopharmaceutical uptake in tumours or metastases is essential and can be performed by positron emitter or single-photon emitter compounds. For these two categories of radiopharmaceuticals,  $\beta^+$  particle emitter [ $^{68}\text{Ga}]\text{Ga}$ -DOTA derivatives for

PET imaging have been developed [67,68], while in the case of  $\gamma$ -emitter compounds, different  $^{99m}\text{Tc}$ -radiopharmaceuticals have been reported for SPECT PCa imaging. In this last case, the possibility of choosing from different synthesis strategies to ensure robust radiolabelling has been the driving force in the development of compounds with improved biodistribution properties. Based on the chemistry of the organometallic fragment  $[^{99m}\text{Tc}][\text{Tc}(\text{CO})_3(\text{H}_2\text{O})_3]^+$ , two promising compounds, MIP-1404 and MIP-1405, both based on an imidazole modification of the PSMA inhibitor, were developed (Figure 9).

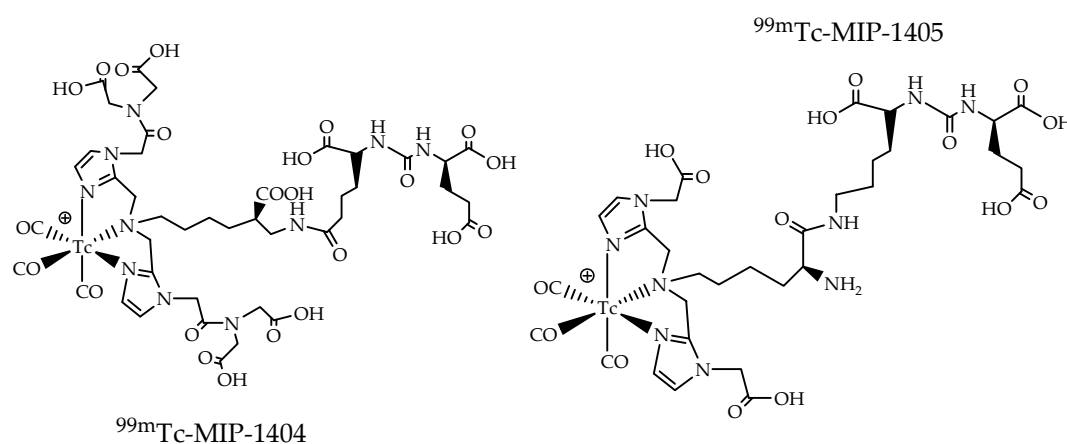


**Figure 9.** The chemical structure of the complexes  $[^{99m}\text{Tc}][\text{Tc}(\text{CO})_3\text{-MIP-1404, MIP-1405}]$ .

The preparation of the metal complexes  $[^{99m}\text{Tc}][\text{Tc}(\text{CO})_3\text{-MIP-1404, MIP-1405}]$  was accomplished using a standard methodology and commercially available IsoLink kits (Covidien, Dublin, Ireland) and the imidazole chelator, which contains three nitrogen atom suitable for binding to the  $^{99m}\text{Tc}(\text{I})$ -tricarbonyl-core. The radiochemical yield of the final radiopharmaceuticals is only 70% and post-labelling purification is needed [69]. Both compounds were used to visualize tumours in PCa and metastases in lymph nodes and bones. In particular, the MIP-1404 compound, also known as  $[^{99m}\text{Tc}]\text{Tc-trofolostat}$ , has demonstrated superior biodistribution properties with low uptake in the kidney and more lesions than MIP-1405 in a phase II clinical trial [58]. The different pharmacokinetics has been attributed to the carboxymethyl group attached to the imidazole. In the MIP-1405 compound there is only a terminal carboxymethyl group on the imidazole moiety, while MIP-1404 has a bis-carboxymethyl amino-2-oxoethyl group linked to each imidazole (see Figure 9).

The technology of  $^{99m}\text{Tc}$ -hydrazinonicotinyl was also applied in the development of a PSMA inhibitor for  $^{99m}\text{Tc}$ -based SPECT. Ferro-Flores et al. [70] reported in vitro and in vivo studies of  $^{99m}\text{Tc}$ -EDDA-HYNIC-iPSMA demonstrating that this radiopharmaceutical could detect tumour and metastases of PCa as well as  $^{68}\text{Ga}$ -PSMA-617.  $^{99m}\text{Tc}$ -EDDA-HYNIC-iPSMA was quickly prepared from a kit with radiochemical yield >95%.

Recently, a new  $^{99m}\text{Tc}$  radiopharmaceutical, known as  $^{99m}\text{Tc}$ -PSMA-I&S (I&S = investigation and surgery), is available for SPECT imaging and radio-guided surgery (RGS) for clinical application in urology [71]. This compound can be produced through a robust and reliable freeze-dried kit, facilitating the on-site production. The radiopharmaceutical is based on the molecule DOTAGA-(3-iodo-y)-f-k-Sub(KuE), in which the DOTA chelator is present to coordinate indium-111.

Due to the limitations associated with the high cost, poor availability, and non-ideal nuclear properties of this radionuclide, a technetium-99m analogue has been proposed. The DOTA chelator, specifically used for indium-111 labelling, has been replaced with the hydrophilic  $\text{MAG}_3$ -analogue  $\text{MAS}_3$  (mercaptoacetyl triserina), with the aim of stably binding the technetium-99m in the V oxidation state (Figure 10). At first, the use of the ease and efficient  $\text{MAG}_3$  labelling procedure allowed the formation of the  $^{99m}\text{Tc}$ - $\text{MAS}_3$ -y-nal-k(Sub-KuE) complex, where the 3-iodo-D-Tyr-D-Phe-sequence in the linker moiety was replaced by a D-Tyr-D-2-Nal-sequence to enhance its interaction with a

remote arene binding site. Then, a second, more stable compound,  $^{99m}\text{Tc}$ -mas<sub>3</sub>-y-nal-k(Sub-KuE), was developed, where all the L-serines in the chelator MAS<sub>3</sub> (2-mercaptoacetyl-L-Ser-L-Ser-L-Ser-), more susceptible to proteolytic degradation, have been replaced with the corresponding D-serine-(mas3) (Figure 10). The high in vivo stability of the resulting  $^{99m}\text{Tc}$ -PSMA-I&S compound represents a major prerequisite for RGS clinical application performed on the day after the tracer injection for practical reasons [71].  $^{99m}\text{Tc}$ -PSMA-I&S is a promising gamma probe that could potentially be used for in vivo intraoperative measurements to facilitate localizing metastases and removing recurrent PCa lesions. A very recent study also demonstrated the feasibility of using a  $^{99m}\text{Tc}$ -PSMA-I&S radiopharmaceutical to guide intraoperative identification and surgical removal of metastatic lymph nodes in PCa patients scheduled for salvage surgery [72]. The PSMA radio-guided surgery essentially involves, first, the selection of patients based on  $^{68}\text{Ga}$ -PSMA-PET results and clinical history, then the injection of  $^{99m}\text{Tc}$ -PSMA-I&S and subsequent SPECT/CT imaging aiming to confirm the technetium uptake in the same lesions of the preoperative gallium-68 compound. Finally, PSMA radio-guided surgery is performed with in vivo and ex vivo gamma probes to reliably identify the metastatic prostate cancer lesions. Figure 11 is a graphical representation of the steps of PSMA radio-guided surgery.

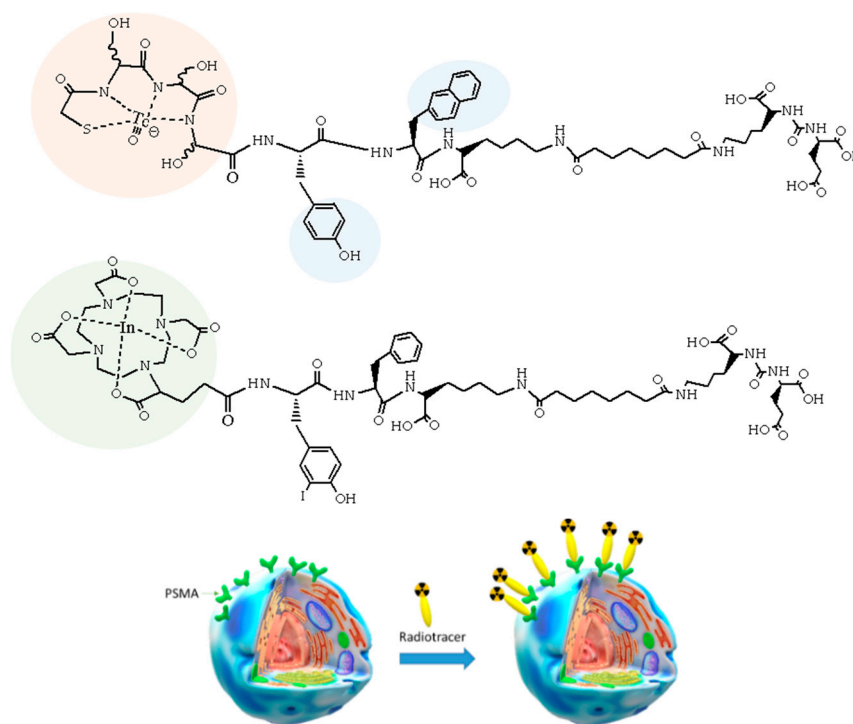


**Figure 10.** The chemical structure of the complexes  $^{111}\text{In}$ -PSMA-I&T and  $^{99m}\text{Tc}$ -MAS<sub>3</sub>/mas<sub>3</sub>-y-nal-k-Sub-KuE, and a graphical representation of the interaction between the radiotracer and PSMA.

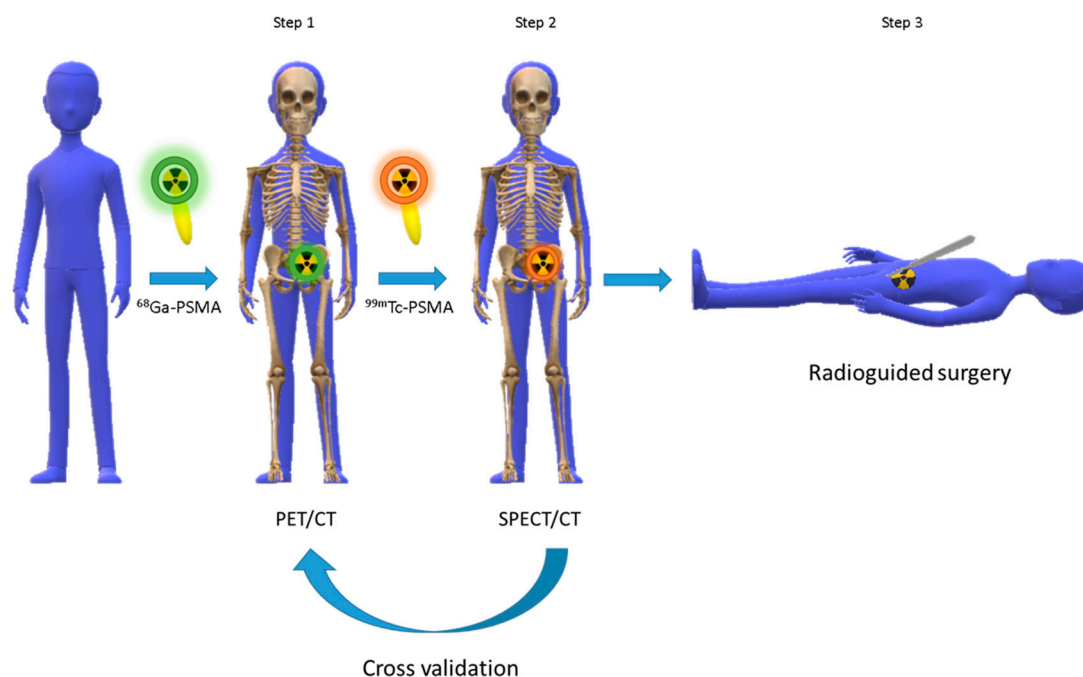


**Figure 11.** The steps of PSMA radio-guided surgery.

## 5. Conclusions

The scientific advances of the last 20 years in the development of chemical approaches dedicated to selectively introducing and stabilizing the metal technetium-99m into a bioactive construct, such as the “ $^{99\text{m}}\text{Tc}$ -metal fragment approach,” have allowed the development of new technetium-99m radiopharmaceuticals for tumour imaging, previously thought to be a prerogative of PET and other radionuclides. The recent impressive results achieved with different PSMA target derivatives, in combination with improvement of the SPECT technology, indicate that  $^{99\text{m}}\text{Tc}$  radiopharmaceuticals are far from obsolete and will continue to play an important and renewed role in nuclear medicine.

**Author Contributions:** Conceptualization, A.B. and L.U.; writing—original draft preparation, P.M.; writing—review and editing, P.M.

**Funding:** This research received no external funding.

**Conflicts of Interest:** The authors declare no conflict of interest.

## References

1. Mankoff, D.A. A definition of molecular imaging. *J. Nucl. Med.* **2007**, *48*, 18N–21N. [[PubMed](#)]
2. Pysz, M.A.; Gambhir, S.S.; Willmann, J.K. Molecular Imaging: Current Status and Emerging Strategies. *Clin. Radiol.* **2010**, *65*, 500–516. [[CrossRef](#)] [[PubMed](#)]
3. Qaim, S.M.; Spahn, I. Development of novel radionuclides for medical applications. *J. Label. Comp. Radiopharm.* **2018**, *61*, 126–140. [[CrossRef](#)] [[PubMed](#)]
4. Boschi, A.; Martini, P.; Uccelli, L.  $^{188}\text{Re(V)}$  Nitrido Radiopharmaceuticals for Radionuclide Therapy. *Pharmaceuticals* **2017**, *10*, 12. [[CrossRef](#)] [[PubMed](#)]
5. Mottaghy, F.M. Current and future aspects of molecular imaging. *Methods* **2009**, *48*, 81–82. [[CrossRef](#)] [[PubMed](#)]
6. Uccelli, L.; Martini, M.; Cittanti, C.; Carnevale, A.; Missiroli, L.; Giganti, M.; Bartolomei, M.; Boschi, A. Therapeutic Radiometals: Worldwide Scientific Literature Trend Analysis (2008–2018). *Molecules* **2019**, *24*, 640. [[CrossRef](#)] [[PubMed](#)]
7. Qaim, S.M. Nuclear data for medical applications: An overview. *Radiochim. Acta* **2001**, *89*, 189–196. [[CrossRef](#)]
8. Boschi, A.; Martini, P.; Janevik-Ivanovska, E.; Duatti, A. The emerging role of copper-64 radiopharmaceuticals as cancer theranostics. *Drug Discov. Today* **2018**, *23*, 1489–1501. [[CrossRef](#)]

9. Bartholoma, M.D.; Louie, A.S.; Valliant, J.F.; Zubieta, J. Technetium and Gallium Derived Radiopharmaceuticals: Comparing and Contrasting the Chemistry of Two Important Radiometals for the Molecular Imaging Era. *Chem. Rev.* **2010**, *110*, 2903–2920. [[CrossRef](#)]
10. Uccelli, L.; Martini, P.; Pasquali, M.; Boschi, A. Monoclonal Antibodies Radiolabeling with Rhenium-188 for Radioimmunotherapy. *BioMed Res. Int.* **2017**, *2017*. [[CrossRef](#)]
11. Rathmann, S.M.; Ahmad, Z.; Slikboer, S.; Bilton, H.A.; Snider, D.P.; Valliant, J.F. The Radiopharmaceutical Chemistry of Technetium-99m. In *Radiopharmaceutical Chemistry*; Lewis, J.S., Windhorst, A.D., Zeglis, B.M., Eds.; Springer Nature Switzerland AG: Cham, Switzerland, 2019; pp. 311–333.
12. Liu, S. Bifunctional coupling agents for radiolabeling of biomolecules and target-specific delivery of metallic radionuclides. *Adv. Drug Deliv. Rev.* **2008**, *60*, 1347–1370. [[CrossRef](#)] [[PubMed](#)]
13. Jurisson, S.S.; Lydon, J.D. Potential Technetium Small Molecule Radiopharmaceuticals. *Chem. Rev.* **1999**, *99*, 2205–2218. [[CrossRef](#)] [[PubMed](#)]
14. Herschman, H.R. Molecular imaging: Looking at problems, seeing solutions. *Science* **2003**, *302*, 605–608. [[CrossRef](#)] [[PubMed](#)]
15. Garcia, E.V.; Faber, T.L. Advances in nuclear cardiology instrumentation: Clinical potential of SPECT and PET. *Curr. Cardiovasc. Imaging Rep.* **2009**, *2*, 230–237. [[CrossRef](#)]
16. IAEA. *Technetium-99m Radiopharmaceuticals: Status and Trends*; IAEA Radioisotopes and Radiopharmaceuticals Series; International Atomic Energy Agency: Vienna, Austria, 2009; No. 1.
17. Alenazy, A.B.; Wells, R.G.; Ruddy, T.D. New solid state cadmium-zinc-telluride technology for cardiac single photon emission computed tomographic myocardial perfusion imaging. *Expert Rev. Med. Devices* **2017**, *14*, 213–222. [[CrossRef](#)] [[PubMed](#)]
18. Molinski, V.J. A review of  $^{99m}\text{Tc}$  generator technology. *Int. J. Appl. Radiat. Isot.* **1982**, *33*, 811–819. [[CrossRef](#)]
19. Uccelli, L.; Martini, P.; Pasquali, M.; Boschi, A. Radiochemical purity and stability of  $^{99m}\text{Tc}$ -HMPAO in routine preparations. *J. Radioanal. Nucl. Chem.* **2017**, *314*, 1177–1181. [[CrossRef](#)]
20. Ross, C.A.; Diamond, W.T. Predictions regarding the supply of  $^{99}\text{Mo}$  and  $^{99m}\text{Tc}$  when NRU ceases production in 2018. *Phys. Can.* **2015**, *71*, 131–138.
21. Opportunities and Approaches for Supplying Molybdenum-99 and Associated Medical Isotopes to Global Markets Proceedings of a Symposium 2018. Available online: <http://www.nap.edu/24909> (accessed on 15 May 2019).
22. Boschi, A.; Martini, P.; Pasquali, M.; Uccelli, L. Recent achievements in Tc-99m radiopharmaceutical direct production by medical cyclotrons. *Drug Dev. Ind. Pharm.* **2017**, *43*, 1402–1412. [[CrossRef](#)]
23. Uzunov, N.; Melendez-Alafort, L.; Bello, M.; Cicoria, G.; Zagni, F.; De Nardo, L.; Selva, A.; Mou, L.; Rossi-Alvarez, C.; Pupillo, G.; et al. Radioisotopic purity and imaging properties of cyclotron-produced  $^{99m}\text{Tc}$  using direct  $^{100}\text{Mo}(p,2n)$  reaction. *Phys. Med. Biol.* **2018**, *63*, 185021. [[CrossRef](#)]
24. Capogni, M.; Pietropaolo, A.; Quintieri, L.; Angelone, M.; Boschi, A.; Capone, M.; Cherubini, N.; De Felice, P.; Dodaro, A.; Duatti, A. 14 MeV Neutrons for  $^{99}\text{Mo}/^{99m}\text{Tc}$  Production: Experiments, Simulations and Perspectives. *Molecules* **2018**, *23*, 1872. [[CrossRef](#)] [[PubMed](#)]
25. Esposito, J.; Bettoni, D.; Boschi, A.; Calderolla, M.; Cisternino, S.; Fiorentini, G.; Keppel, G.; Martini, P.; Maggiore, M.; Mou, L.; et al. LARAMED: A Laboratory for Radioisotopes of Medical Interest. *Molecules* **2019**, *24*, 20. [[CrossRef](#)] [[PubMed](#)]
26. Jang, J.; Yamamoto, M.; Uesaka, M. Design of an X-band electron linear accelerator dedicated to decentralized  $^{99}\text{Mo}/^{99m}\text{Tc}$  supply: From beam energy selection to yield estimation. *Phys. Rev. Accel. Beams* **2017**, *20*, 104701. [[CrossRef](#)]
27. Martini, P.; Boschi, A.; Cicoria, G.; Zagni, F.; Corazza, A.; Uccelli, L.; Pasquali, M.; Pupillo, G.; Marengo, M.; Loriggiola, M.; et al. In-House Cyclotron Production of High-Purity Tc-99m and Tc-99m Radiopharmaceuticals. *Appl. Radiat. Isot.* **2018**, *139*, 325–331. [[CrossRef](#)] [[PubMed](#)]
28. Rovaisn, M.R.A.; Aardaneh, K.; Aslani, G.; Rahiminejad, A.; Yousefi, K.; Boulou, F. Assessment of the direct cyclotron production of  $^{99m}\text{Tc}$ : An approach to crisis management of  $^{99m}\text{Tc}$  shortage. *Appl. Radiat. Isot.* **2016**, *112*, 55–61. [[CrossRef](#)]
29. Lei, K.; Rusckowski, M.; Chang, F.; Qu, T.; Mardirossian, G.; Hnatowich, D.J. Technetium-99m antibodies labeled with MAG3 and SHNH: An In Vitro and animal In Vivo comparison. *Nucl. Med. Biol.* **1996**, *23*, 917–922. [[CrossRef](#)]

30. Goodbody, A.; Pollak, A. Peptide-Chelator Conjugates for Diagnostic Imaging. PCT International Application W09603427, 8 February 1996.
31. Van Domselaar, G.H.; Okarvi, S.M.; Fanta, M.; Suresh, M.R.; Wishart, D.S. Synthesis and  $^{99m}\text{Tc}$ -labelling of bz-MAG3-triprolinyl-peptides, their radiochemical evaluation and in vitro receptor-binding. *J. Label. Compd. Radiopharm.* **2000**, *43*, 1193–1204. [[CrossRef](#)]
32. Zhu, Z.; Wang, Y.; Zhang, Y.; Liu, G.; Liu, N.; Rusckowski, M.; Hnatowich, D.J. A novel and simplified route to the synthesis of  $\text{N}_3\text{S}$  chelators for  $^{99m}\text{Tc}$  labeling. *Nucl. Med. Biol.* **2001**, *28*, 703–708. [[CrossRef](#)]
33. Abram, U.I.; Alberto, R. Technetium and rhenium-coordination chemistry and nuclear medical applications. *J. Braz. Chem. Soc.* **2006**, *17*, 1486–1500. [[CrossRef](#)]
34. Skaddan, M.B.; Wust, F.R.; Jonson, S.; Syhre, R.; Welch, M.J.; Spies, H.; Katzenellenbogen, J.A. Radiochemical synthesis and tissue distribution of Tc-99m-labeled 7 $\alpha$ -substituted estradiol complexes. *Nucl. Med. Biol.* **2000**, *27*, 269–278. [[CrossRef](#)]
35. Shunichi, O.; Ploessl, K.; Kung, M.P.; Stevenson, D.A. Small and Neutral TcvO BAT, Bisaminoethanethiol ( $\text{N}_2\text{S}_2$ ) Complexes for Developing New Brain Imaging Agents. *Nucl. Med. Biol.* **1998**, *25*, 135–140.
36. Hnatowich, D.J.; Qu, T.; Chang, F.; Ley, A.C.; Ladner, R.C.; Rusckowski, M. Labeling peptides with technetium-99m using a bifunctional chelator of a N-hydroxysuccinimide ester of mercaptoacetyltriglycine. *J. Nucl. Med.* **1998**, *39*, 56–64. [[PubMed](#)]
37. Hom, K.R.; Chi, D.Y.; Katzenellenbogen, J.A. Heterodimeric Bis (Amino Thiol) Complexes of Oxorhenium (V) That Mimic the Structure of Steroid Hormones. Synthesis and Stereochemical Issues. *J. Org. Chem.* **1996**, *61*, 2624–2631. [[CrossRef](#)] [[PubMed](#)]
38. Mozley, P.D.; Schneider, J.S.; Acton, P.D.; Plossl, K.; Stern, M.B.; Siderowf, A.; Leopold, N.A.; Li, P.Y.; Alavi, A.; Kung, H.F. Binding of [ $^{99m}\text{Tc}$ ]TRODAT-1 to dopamine transporters in patients with Parkinson's disease and in healthy volunteers. *J. Nucl. Med.* **2000**, *41*, 584–589. [[PubMed](#)]
39. Kung, H.F.; Kung, M.P.; Wey, S.P.; Lin, K.J.; Yen, T.C. Clinical acceptance of a molecular imaging agent: A long march with [ $^{99m}\text{Tc}$ ]TRODAT. *Nucl. Med. Biol.* **2007**, *34*, 787–789. [[CrossRef](#)] [[PubMed](#)]
40. Kung, H.F.; Kim, H.J.; Kung, M.P.; Meegalla, S.K.; Plössl, K.; Lee, H.K. Imaging of dopamine transporters in humans with technetium-99m TRODAT-1. *Eur. J. Nucl. Med.* **1996**, *23*, 1527–1530. [[CrossRef](#)] [[PubMed](#)]
41. Menda, Y.; Kahn, D. Somatostatin receptor imaging of non-small cell lung cancer with  $^{99m}\text{Tc}$  depreotide. *Semin. Nucl. Med.* **2002**, *32*, 92–96. [[CrossRef](#)]
42. Bååth, M.; Kölbeck, K.G.; Danielsson, R. Somatostatin receptor scintigraphy with  $^{99m}\text{Tc}$ -Depreotide (NeoSpect) in discriminating between malignant and benign lesions in the diagnosis of lung cancer: A pilot study. *Acta Radiol.* **2004**, *45*, 833–839. [[CrossRef](#)]
43. Schwartz, D.A.; Abrams, M.J.; Hauser, M.M.; Gaul, F.E.; Larsen, S.K.; Rauh, D.; Zubieta, J. Preparation of hydrazino-modified proteins and their use for the synthesis of technetium-99m-protein conjugates. *Bioconjug. Chem.* **1991**, *2*, 333–336. [[CrossRef](#)]
44. Rose, D.J.; Maresca, K.P.; Nicholson, T.; Davison, A.; Jones, A.G.; Babich, J.; Fischman, A.; Graham, W.; De Bord, J.R.D.; Zubieta, J. Synthesis and Characterization of Organohydrazino Complexes of Technetium, Rhenium, and Molybdenum with the  $\{\text{M}(\eta^1\text{-HxNNR})(\eta^2\text{-HyNNR})\}$  Core and Their Relationship to Radiolabeled Organohydrazine-Derivatized Chemotactic Peptides with Diagnostic Applications. *Inorg. Chem.* **1998**, *37*, 2701–2716. [[CrossRef](#)]
45. Liu, S. 6-Hydrazinonicotinamide Derivatives as Bifunctional Coupling Agents for  $^{99m}\text{Tc}$ -Labeling of Small Biomolecules. *Top. Curr. Chem.* **2008**, *252*, 117–153.
46. Liepe, K.; Becker, A.  $^{99m}\text{Tc}$ -Hynic-TOC imaging in the diagnostic of neuroendocrine tumors. *World J. Nucl. Med.* **2018**, *17*, 151–156. [[CrossRef](#)] [[PubMed](#)]
47. Trogrlic, M.; Težak, S. Incremental value of  $^{99m}\text{Tc}$ -HYNIC-TOC SPECT/CT over whole-body planar scintigraphy and SPECT in patients with neuroendocrine tumours. *Nuklearmedizin* **2017**, *56*, 97–107.
48. Czepczyński, R.; Gryczyńska, M.; Ruchała, M.  $^{99m}\text{Tc}$ -EDDA/HYNIC-TOC in the diagnosis of differentiated thyroid carcinoma refractory to radioiodine treatment. *Nucl. Med. Rev. Cent. East. Eur.* **2016**, *19*, 67–73. [[CrossRef](#)] [[PubMed](#)]
49. Bangard, M.; Béhé, M.; Guhlke, S.; Otte, R.; Bender, H.; Maecke, H.R.; Biersack, H.J. Detection of somatostatin receptor-positive tumours using the new  $^{99m}\text{Tc}$ -tricine-HYNIC-D-Phe1-Tyr3-octreotide: First results in patients and comparison with  $^{111}\text{In}$ -DTPA-D-Phe1-octreotide. *Eur. J. Nucl. Med.* **2000**, *27*, 628–637. [[CrossRef](#)]

50. Boschi, A.; Duatti, A.; Uccelli, L. Development of Technetium-99m and Rhenium-188 Radiopharmaceuticals Containing a Terminal Metal–Nitrido Multiple Bond for Diagnosis and Therapy. *Top. Curr. Chem.* **2005**, *252*, 85–115.
51. Cazzola, E.; Benini, E.; Pasquali, M.; Mirtschink, P.; Walther, M.; Pietzsch, H.J.; Uccelli, L.; Boschi, A.; Bolzati, C.; Duatti, A. Labeling of fatty acid ligands with the strong electrophilic metal fragment  $[^{99m}\text{Tc}(\text{N})(\text{PNP})]^{2+}$  (PNP = diphosphane ligand). *Bioconjug. Chem.* **2008**, *19*, 450–460. [[CrossRef](#)]
52. Bu, L.; Li, R.; Jin, Z.; Wen, X.; Liu, S.; Yang, B.; Shen, B.; Chen, X. Evaluation of  $(99\text{m})\text{TcN-MPO}$  as a new myocardial perfusion imaging agent in normal dogs and in an acute myocardial infarction canine model: Comparison with  $(99\text{m})\text{Tc-sestamibi}$ . *Mol. Imaging Biol.* **2011**, *13*, 121–127. [[CrossRef](#)]
53. Zheng, Y.; Ji, S.; Tomaselli, E.; Liu, S. Development of kit formulations for  $(99\text{m})\text{TcN-MPO}$ : A cationic radiotracer for myocardial perfusion imaging. *J. Label. Comp. Radiopharm.* **2014**, *57*, 584–592. [[CrossRef](#)]
54. Boschi, A.; Uccelli, L.; Duatti, A.; Bolzati, C.; Refosco, F.; Tisato, F.; Romagnoli, R.; Baraldi, P.G.; Varani, K.; Borea, P.A. Asymmetrical Nitrido Tc-99m Heterocomplexes as Potential Imaging Agents for Benzodiazepine Receptors. *Bioconjug. Chem.* **2003**, *14*, 1279–1288.
55. Bolzati, C.; Mahmood, A.; Malago, E.; Uccelli, L.; Boschi, A.; Jones, A.G.; Refosco, F.; Duatti, A.; Tisato, F. The  $[^{99m}\text{Tc}(\text{N})(\text{PNP})]^{2+}$  Metal Fragment: A Technetium-Nitrido Synthone for Use with Biologically Active Molecules. The N-(2-Methoxyphenyl)piperazyl-cysteine Analogues as Examples. *Bioconjug. Chem.* **2003**, *14*, 1231–1242. [[CrossRef](#)] [[PubMed](#)]
56. Alberto, R.; Schibli, R.; Schubiger, A.P.; Abram, U.; Pietzsch, H.J.; Johannsen, B. First application of *fac*- $[^{99m}\text{Tc}(\text{OH}_2)_3(\text{CO})_3]^+$  in bioorganometallic chemistry: Design, structure, and In Vitro affinity of a 5-HT1A receptor ligand labeled with  $^{99m}\text{Tc}$ . *J. Am. Chem. Soc.* **1999**, *121*, 6076–6077. [[CrossRef](#)]
57. Bilton, H.A.; Ahmad, Z.; Janzen, N.; Czorny, S.; Valliant, J.F. Preparation and evaluation of  $^{99m}\text{Tc}$ -labeled tridentate chelates for pre-targeting using bioorthogonal chemistry. *J. Vis. Exp.* **2017**, *120*, e55188.
58. Goffin, K.E.; Joniau, S.; Tenke, P.; Slawin, K.; Klein, E.A.; Stambler, N.; Strack, T.; Babich, J.; Armor, T.; Wong, V. Phase 2 study of  $^{99m}\text{Tc}$ -trofolostat SPECT/CT to identify and localize prostate cancer in intermediate- and high-risk patients undergoing radical prostatectomy and extended pelvic LN dissection. *J. Nucl. Med.* **2017**, *58*, 1408–1413. [[CrossRef](#)] [[PubMed](#)]
59. Alberto, R.; Schibli, R.; Egli, A.; Schubiger, A.P.; Abram, U.; Kaden, T.A. A Novel organometallic aqua complex of technetium for the labeling of biomolecules: Synthesis of  $[^{99m}\text{Tc}(\text{OH}_2)_3(\text{CO})_3]^+$  from  $[^{99m}\text{TcO}_4]^-$  in aqueous solution and its reaction with a bifunctional ligand. *J. Am. Chem. Soc.* **1998**, *120*, 7987–7988. [[CrossRef](#)]
60. Lipowska, M.; Klenc, J.; Taylor, A.T.; Marzilli, L.G. *fac*- $^{99m}\text{Tc/Re}$ -tricarboxyl complexes with tridentate aminocarboxyphosphonate ligands: Suitability of the phosphonate group in chelate ligand design of new imaging agents. *Inorganica Chim. Acta* **2019**, *486*, 529–537. [[CrossRef](#)] [[PubMed](#)]
61. Mindt, T.L.; Struthers, H.; Brans, L.; Anguelov, T.; Schweinsberg, C.; Maes, V.; Tourwé, D.; Schibli, R. “Click to chelate”: Synthesis and installation of metal chelates into biomolecules in a single step. *J. Am. Chem. Soc.* **2006**, *128*, 15096–15097. [[CrossRef](#)] [[PubMed](#)]
62. Benešová, M.; Schäfer, M.; Bauder-Wüst, U.; Afshar-Oromieh, A.; Kratochwil, C.; Mier, W.; Haberkorn, U.; Kopka, K.; Eder, M. Preclinical evaluation of a tailor-made DOTA-conjugated PSMA inhibitor with optimized linker moiety for imaging and endoradiotherapy of prostate cancer. *J. Nucl. Med.* **2015**, *56*, 914–920. [[CrossRef](#)]
63. Violet, J.; Jackson, P.; Ferdinandus, J.; Sandhu, S.; Akhurst, T.; Iravani, A.; Kong, G.; Kumar, A.R.; Thang, S.P.; Eu, P.; et al. Dosimetry of  $^{177}\text{Lu}$ -PSMA-617 in Metastatic Castration-Resistant Prostate Cancer: Correlations between Pretherapeutic Imaging and Whole-Body Tumor Dosimetry with Treatment Outcomes. *J. Nucl. Med.* **2019**, *60*, 517–523. [[CrossRef](#)]
64. Baum, R.P.; Kulkarni, H.R.; Schuchardt, C.; Singh, A.; Wirtz, M.; Wiessalla, S.; Schottelius, M.; Mueller, D.; Klette, I.; Wester, H.J. Lutetium-177 PSMA radioligand therapy of metastatic castration-resistant prostate cancer: Safety and efficacy. *J. Nucl. Med.* **2016**, *57*, 1006–1013. [[CrossRef](#)]
65. Rahbar, K.; Schmidt, M.; Heinzl, A.; Eppard, E.; Bode, A.; Yordanova, A.; Claesener, M.; Ahmadzadehfar, H. Response and tolerability of a single dose of  $^{177}\text{Lu}$ -PSMA-617 in patients with metastatic castration-resistant prostate cancer: A multicenter retrospective analysis. *J. Nucl. Med.* **2016**, *57*, 1334–1338. [[CrossRef](#)] [[PubMed](#)]

66. Kratochwil, C.; Giesel, F.L.; Stefanova, M.; Benešová, M.; Bronzel, M.; Afshar-Oromieh, A.; Mier, W.; Eder, M.; Kopka, K.; Haberkorn, U. PSMA-targeted radionuclide therapy of metastatic castration-resistant prostate cancer with Lu-177 labeled PSMA-617. *J. Nucl. Med.* **2016**, *57*, 1170–1176. [[CrossRef](#)] [[PubMed](#)]
67. Eder, M.; Neels, O.; Müller, M.; Bauder-Wüst, U.; Remde, Y.; Schäfer, M.; Hennrich, U.; Eisenhut, M.; Afshar-Oromieh, A.; Haberkorn, U.; et al. Novel preclinical and radiopharmaceutical aspects of [<sup>68</sup>Ga] Ga-PSMA-HBED-CC: A new PET tracer for imaging of prostate cancer. *Pharmaceuticals* **2014**, *7*, 779–796. [[CrossRef](#)] [[PubMed](#)]
68. Afshar-Oromieh, A.; Haberkorn, U.; Schlemmer, H.; Fenchel, M.; Eder, M.; Eisenhut, M.; Hadaschik, B.A.; Kopp-Schneider, A.; Röthke, M. Comparison of PET/CT and PET/MRI hybrid systems using a <sup>68</sup>Ga-labelled PSMA ligand for the diagnosis of recurrent prostate cancer: Initial experience. *Eur. J. Nucl. Med. Mol. Imaging* **2014**, *41*, 887–897. [[CrossRef](#)] [[PubMed](#)]
69. Hillier, S.M.; Maresca, K.P.; Lu, G.; Merkin, R.D.; Marquis, J.C.; Zimmerman, C.N.; Eckelman, W.C.; Joyal, J.L.; Babich, J.W. <sup>99m</sup>Tc-labeled small-molecule inhibitors of prostate-specific membrane antigen for molecular imaging of prostate cancer. *J. Nucl. Med.* **2013**, *54*, 1369–1376. [[CrossRef](#)] [[PubMed](#)]
70. Ferro-Flores, G.; Luna-Gutiérrez, M.; Ocampo-García, B.; Santos-Cuevas, C.; Azorín-Vega, E.; Jiménez-Mancilla, N.; Orocio-Rodríguez, E.; Davanzo, J.; García-Pérez, F.O. Clinical translation of a PSMA inhibitor for <sup>99m</sup>Tc-based SPECT. *Nucl. Med. Biol.* **2017**, *48*, 36–44. [[CrossRef](#)] [[PubMed](#)]
71. Robu, S.; Schottelius, M.; Eiber, M.; Maurer, T.; Gschwend, J.; Schwaiger, M.; Wester, H.J. Preclinical Evaluation and First Patient Application of <sup>99m</sup>Tc-PSMA-I&S for SPECT Imaging and Radioguided Surgery in Prostate Cancer. *J. Nucl. Med.* **2017**, *58*, 235–242.
72. Maurer, T.; Robu, S.; Schottelius, M.; Schwamborn, K.; Rauscher, I.; van den Berg, N.S.; van Leeuwen, F.W.B.; Haller, B.; Horn, T.; Heck, M.M.; et al. <sup>99m</sup>Technetium-Based Prostate-Specific Membrane Antigen-Radioguided Surgery in Recurrent Prostate Cancer. *Eur. Urol.* **2019**, *75*, 659–666. [[CrossRef](#)]



© 2019 by the authors. Licensee MDPI, Basel, Switzerland. This article is an open access article distributed under the terms and conditions of the Creative Commons Attribution (CC BY) license (<http://creativecommons.org/licenses/by/4.0/>).